Organic Process Research & Development

ARTICLE

pubs.acs.org/OPRD

Application of Internal Seeding and Temperature Cycling for Reduction of Liquid Inclusion in the Crystallization of RDX

Jun-Woo Kim,[†] Jae-Kyeong Kim,[†] Hyoun-Soo Kim,[‡] and Kee-Kahb Koo*[,†]

[†]Department of Chemical and Biomolecular Engineering, Sogang University, Seoul 121-742, Korea

[‡]Agency for Defense Development, Daejeon 305-600, Korea

ABSTRACT: In the cooling crystallization of cyclotrimethylene trinitramine (RDX) from γ-butyrolactone, an internal seeding method combined with temperature cycling, was applied to suppress liquid inclusion and improve particle size and size distribution for RDX at initial saturation temperatures of 60−80 °C. The process parameters including initial cooling rate, the range of the temperature cycle, and recooling rate during crystal growth period were determined based on direct measurements of size and amount of liquid inclusion of RDX crystals. Crystal size was measured by a dynamic light scattering particle size analyzer. Liquid inclusion was characterized in mass and area measurement based content by gas chromatography and matching refractive index method combined with image analysis. In the present work, RDX particles with average crystal sizes of 169.0−322.0 μm and inclusion area contents of 4.4−5.3% were obtained. Those values imply that the crystal quality of RDX is much improved compared with those of commercial RDXs such as Hanwha-RDX (conventional grade; average crystal size of 158.0 μm and inclusion area content of 9.3%) and I-RDX (reduced sensitivity grade; average crystal size of 218.0 μm and inclusion area content of 5.0%). For instance, the average crystal size of RDX obtained from a saturated solution at 70 °C by the present method is 290.3 μm, which was much larger than that of I-RDX, but the inclusion area content was about 4.6%, which was even lower than that of I-RDX.

1. INTRODUCTION

Seeding is a typical method to control the size of product crystals by inhibiting undesired nucleation in industrial crystallization.[1−3] In spite of the apparent advantages of seeding, this technique may not be feasible every time due to operational problems or safety concerns such as unavailability of ports for addition of seeds, or potential additional hazards associated with operator's exposure to toxic particles, solvents, and dust explosion.[4,5] When external seeding is inappropriate to apply or the material does not need seeding to crystallize out, internal seeding may be utilized.

In contrast to an external seeding system, in an internal seeding system, fine particles generated by primary nucleation in a crystallizer are used as the seeds.[6] If nucleation is induced by cooling, a slight heating step, which is known as fines destruction or fines dissolution, is often used to control the number of particles. Fines dissolution is quite easy to perform and very efficient in giving large sized crystals and a narrow crystal size distribution (CSD).[7−9] After slight heating, subsequent recooling is applied for growth of the remaining seed crystals. This combined process of heating and cooling is known as a temperature cycling process.

In situ techniques such as attenuated total reflectance Fourier transform infrared (ATR-FTIR) spectroscopy and focused beam reflectance measurement (FBRM) have been shown to successfully aid the internal seeding and temperature cycling process.[10−17] In situ ATR-FTIR spectroscopy was employed for monitoring the concentration inside the crystallizer in the internal seeding processes combined with temperature cycle.[10−12] Chew et al. also reported an internal seeding process combined with single temperature cycle, but they used coefficient of variance of chord length, which was obtained from FBRM, to optimize the range of the heating.[13] Doki et al. demonstrated that FBRM is very useful to maintain the relative crystal population during temperature cycling.[14] Abu Bakar et al. showed that FBRM-assisted temperature cycling is effective to control polymorphic purity as well as size uniformity of crystals compared with linear cooling crystallization.[15] More recent advanced studies on in situ crystallization have also reported that the combination methods of heating/cooling and solvent/antisolvent addition are effective to improve CSD, even if operating temperature profiles are not predetermined.[16,17]

In the batch crystallization of cyclotrimethylene trinitramine (RDX; $C_3H_6N_6O_6$, orthorhombic, *Pbca*, $a = 13.182$ Å, $b = 11.574$ Å, $c = 10.709$ Å, $Z = 8$)[18] from γ-butyrolactone, it has been observed that liquid inclusion rapidly occurs at the initial stage of crystallization.[19] Liquid inclusion exerts deleterious effects on the manufacturing, safe storage, and handling of crystals, such as phase transition, caking, compaction, sintering, and chemical stability. In particular, it has been reported that the liquid inclusion area in the crystalline explosive materials such as RDX acts as the specific region in which a decomposition reaction is readily initiated.[20−25] A commercial RDX with a lower level of liquid inclusion, known as a reduced sensitivity RDX (RS-RDX), was demonstrated to show reduced shock sensitivity when it is incorporated in cast cure and plastic bonded explosives.[26] Therefore, a study on suppression of occurrence of liquid inclusion during crystallization of high-energetic materials has been extensively made.[19,21,26,27]

In the present work, batch cooling crystallization of RDX from γ-butyrolactone with an internal seeding technique combined with temperature cycling was performed to produce RDX crystals with liquid inclusion as low and crystal size as large as

Received: December 17, 2010
Published: March 29, 2011

possible. Although the study on RDX crystallization with the internal seeding method combined with temperature cycling has not appeared to date, it would be expected that the temperature cycling can be a good method to reduce liquid inclusion. This is because the temperature cycling generally involves a delicate temperature control during the initial stage of crystallization in which a large part of liquid inclusions occurred due to the rapid crystal growth.[19,28]

Operating parameters such as cooling rates and the range of the temperature cycle were optimized monitoring crystal size, solvent content, and the number of particle counts obtained from FBRM. Crystal size was measured by using a dynamic light scattering particle size analyzer. Liquid inclusion was characterized by mass and area measurement-based content by GC-FID (gas chromatograph-flame ionization detector) and matching refractive index method combined with image analysis, respectively. In situ monitoring by FBRM was carried out to monitor the crystallization conditions such as the onset of nucleation, stabilization of nucleation and dissolution, and the relative number of dissolved particles.[13−17,29] RDX crystals produced in the present work were compared and discussed with two commercial grade RDXs.

2. EXPERIMENTAL SECTION

2.1. Materials. A conventional grade RDX (99.9%, Hanwha-RDX) was supplied by Hanwha Co., Korea. All samples of Hanwha-RDX were used without further purification. I-RDX produced by Eurenco (France) was selected as a RS-RDX for the comparison with RDX obtained in the present work.

Commercial grade γ-butyrolactone (99+%, Aldrich, USA) was used as the solvent for RDX. In the measurement of solvent (γ-butyrolactone) concentration by GC-FID (Agilent, HP 6890 series, USA), acetonitrile (99.8%, Aldrich, USA) and toluene (99.8%, Aldrich, USA) were used as a diluent and an internal standard, respectively. The triple-distilled water used was produced by a distillation apparatus (Younglin, Ultra 370 series, Korea).

2.2. Experimental Apparatus. A double-jacketed glass crystallizer (100 mL) was employed for the RDX crystallization. The temperature of the crystallizer was controlled within ±0.1 °C by a thermostat (Polyscience, model 9710, USA) and recorded every 5 s using a control software written in LabVIEW. RDX solution was stirred by a Teflon-coated magnetic bar (diameter: 60 mm). The agitation speed of 250 rpm was chosen to suspend crystals with no generation of bubbles due to vortex formation during crystallization. In those conditions, any ground or broken crystals were not observed. Number based chord length distribution of RDX crystals was monitored by FBRM (Lasentec, S400A, USA) during the entire crystallization process. The position and orientation of the probe were chosen according to the standard recommendation to avoid particles adhering to the probe: the probe of FBRM was placed 10 mm above the stirrer, and the probe window faced at a 30° angle to the horizontal and into the direction of stirrer rotation and flow.

The RDX suspension taken from the crystallizer was filtered over a jacketed glass filter funnel with an aspirator. To prevent undesired crystal growth and nucleation, the temperature of the glass filter funnel was kept the same as that of the crystallizer by a thermostat. The filtered RDX crystals were washed with triple-distilled water three times and then dispersed onto a Petri dish. Collection of samples from a filter funnel was carefully made with an antistatic spoon and spatula made of polytetrafluoroethylene (PTFE). The RDX crystals on a Petri dish were dried in a vacuum oven with phosphorus pentoxide as a drying agent at reduced pressure less than 0.1 in Hg for 48 h. The temperature inside the vacuum oven was maintained at 25 °C. The weight of the sample after 12 h drying was measured to no change.

Table 1. Solubility Data of RDX in γ-Butyrolactone

temp (°C)	solubility (g RDX/g solvent)
20	0.134
30	0.162
40	0.196
50	0.238
60	0.290
70	0.355
80	0.436
90	0.540
100	0.658

2.3. Batch Cooling Crystallization. The solubility data of RDX in γ-butyrolactone, which were obtained in our previous work, are presented in Table 1.[19] The expression reflecting the influence of temperature on solubility was correlated with an exponential function given by eq 1.

$$C^* = e^{(a + bT)} \quad (1)$$

where C^* and T denote the solubility of RDX (g RDX/g solvent) and temperature (°C), respectively. The parameters a and b were −2.4438 and 0.02024, respectively, and the correlation coefficient R^2 was 0.99978.

Saturated solutions of RDX/γ-butyrolactone at temperatures of 60, 70, and 80 °C were prepared referring to the solubility data. The solutions were kept at a temperature 5 °C higher than the saturation temperature with a stabilization time of 30 min and cooled to the saturation temperature. And then the cooling crystallization with internal seeding and temperature cycling were performed. Figure 1 shows the operating profiles optimized at each saturation temperature and detailed data are given in Table 2. In this figure, it can be said that period A−E is the nucleation and control stage of internal seeds and period E−G is the crystal growth stage.

Those temperature profiles (cooling rate at period A−B, temperature increase at period C−D, and cooling rate at period E−F) were determined from two-step experiments: First, the experiment for the determination of cooling rate at period A−B was carried out. When the initial saturated solution (point A) was cooled, primary nucleation at a certain temperature was detected by a rapid increase in the total number of counts with FBRM. As soon as the total number of counts indicated about 50 counts/s, cooling was stopped (point B) and the solution was stabilized for 30 min (period B−C) at which point primary nucleation was assumed to be complete (point C). The maximum undercooling limit, which is directly related to the maximum allowable supersaturation, mainly depends on the cooling rate.[30,31] Therefore, the crystal quality of th final product is strongly influenced by the cooling rate before nucleation. To determine the appropriate cooling rate at period A−B, the experiments with cooling rates ranging from 0.1 to 1.5 °C/min were carried out and sample crystals at point C were analyzed. In the case of large-scale

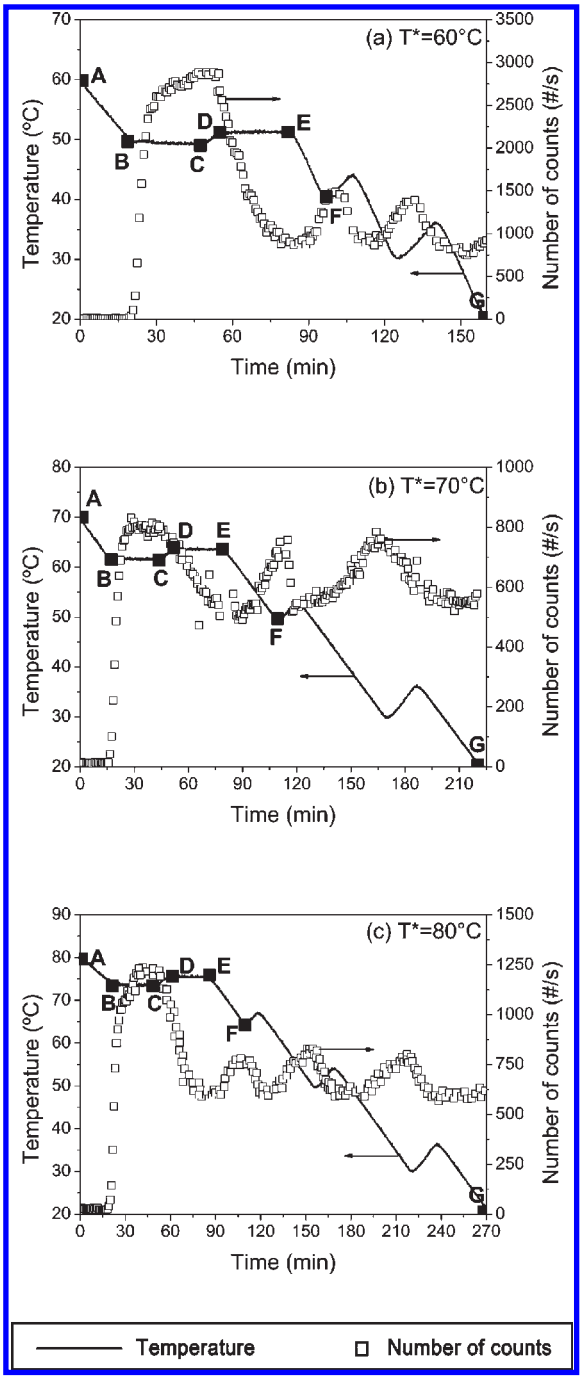

Figure 1. Operating profiles of the batch cooling crystallization of RDX by internal seeding combined with temperature cycling.

experiments in which thermal inertia may not be negligible, further study on the relationship between reactor scale and thermal inertia would be required.

Second, the degree of temperature increase at period C−D and cooling rate at period E−F were determined by the following procedure. After initial cooling with optimized cooling rate and stabilization of nucleation, the solution was heated with a ramping rate of 0.5 deg/min (period C−D) to dissolve fine particles followed by 30 min of stabilization (period D−E) by which dissolution of fines was assumed to be complete. And then linear cooling was introduced (period E−F) again. Here, two

Table 2. Operating Variables of RDX Crystallization with Internal Seeding and Temperature Cycling at the Saturation Temperature of 60, 70, and 80 °C

initial saturation temp (°C)	cooling rate at period A−B (deg/min)	deg of heating at period C−D (°C)	cooling rate at period E−F (deg/min)
60	0.5	2.0	1.0
70	0.5	2.0	0.5
80	0.3	2.0	0.5

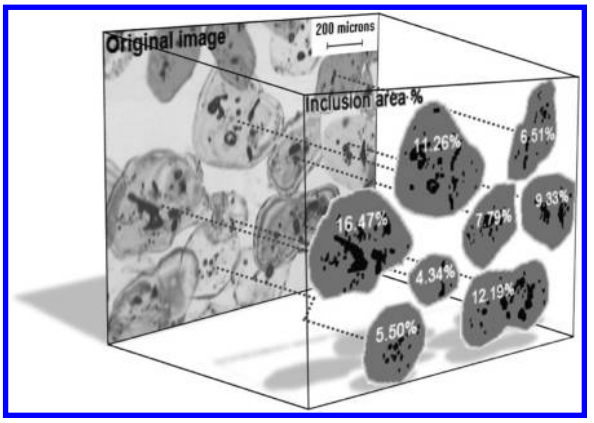

Figure 2. Schematic diagram of image processing for the optical micrograph with matching refractive index.

parameters (degree of temperature increase at period C−D and cooling rate at period E−F) were considered together because reheating (period C−D) is just for the control of the amount of seeds and crystal quality is evaluated after the additional cooling stage (period E−F). In general, when the amount of seeds is decreased by heating, larger crystals are finally obtained. However, a higher growth rate is induced and subsequently enhances the occurrence of liquid inclusion. Therefore, assessment of crystal quality should be carried out after the full temperature cycle. In the present experiments, 24 experiments with 6 levels of temperature increase at period C−D (0 (no heating), 1, 2, 3, 4, 5 °C) and 4 levels of cooling rate at period E−F (0.1, 0.5, 1.0, and 1.5 deg/min) were carried out to optimize temperature profiles at period C−D−E−F.

To obtain the narrow crystal size distribution of RDX, the temperature cycling steps were introduced during the crystal growth stage. When the total number of counts was about 1.5 times that at point E, the reheating process with heating rate of 0.5 deg/min was started until the number of counts returned to that of the initial internal seed crystals, and then the solution was cooled again with optimized cooling rate at period E−F. In this period, the temperature profile was determined by using only the target number of counts/s measured by FBRM. The final temperature of all experiments was 20 °C (point G). For comparison, linear cooling crystallizations of RDX with cooling rate of 1.0 deg/min were performed at saturation temperatures of 50 to 100 °C.

2.4. Characterization of RDX and Liquid Inclusion. The volume weighted mean diameter, $D[4,3]$, was measured by a particle size analyzer (Malvern, Mastersizer 2000, UK). Solvent (γ-butyrolactone) content included in RDX crystals was measured

dx.doi.org/10.1021/op100334y |*Org. Process Res. Dev.* 2011, 15, 602–609

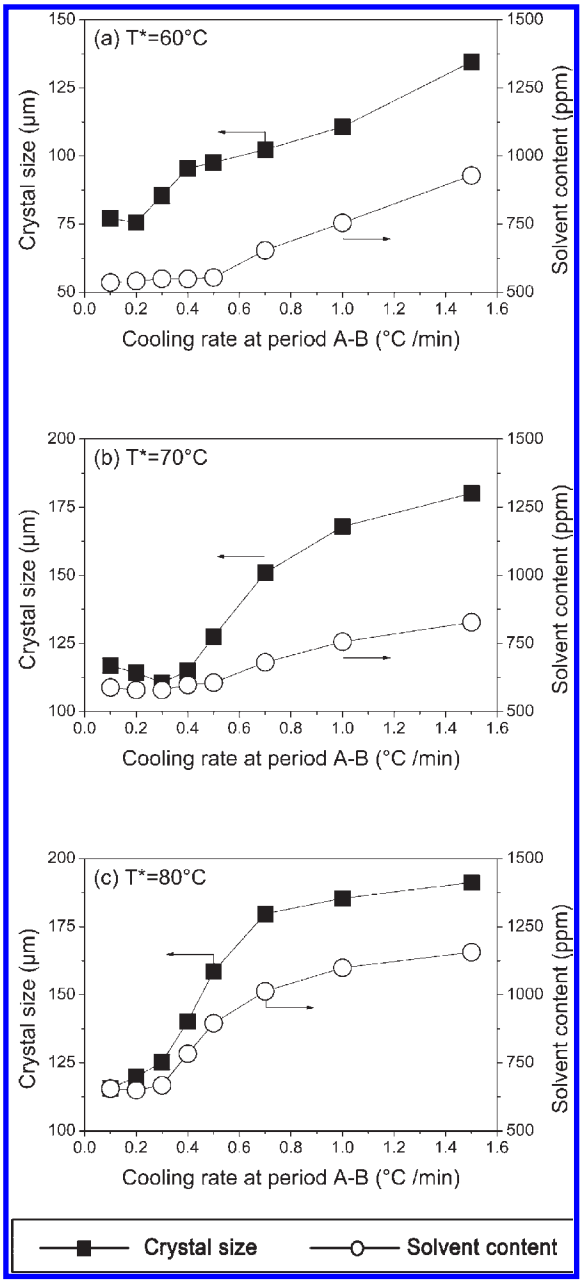

Figure 3. Size and solvent content of RDX crystals taken at point C with various cooling rates at period A−B.

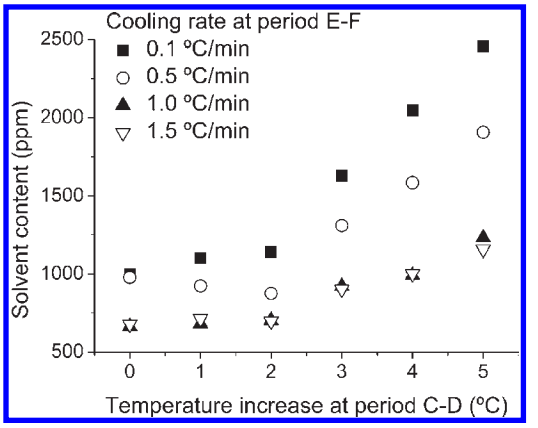

Figure 4. Solvent content of RDX crystals taken at point F with various temperature increases at period C−D and cooling rates at period E−F (initial saturation temperature: 70 °C).

by using a GC-FID. Liquid inclusion was also observed by the matching refractive index method.[32−34] Images observed by optical microscopy were treated by the ternary image processing of white (background region), gray (crystal region), and black (inclusion region), and the average inclusion area of RDX was estimated, as shown in Figure 2. The range of RSD (relative standard deviation) was 1.1−11.6% for GC-FID analysis and 4.3−13.3% for image analysis with matching refractive index, respectively. Details of those characterization techniques on liquid inclusion are given elsewhere.[19]

3. RESULTS AND DISCUSSION

3.1. Optimization of Operating Variables. Figure 3 represents the crystal size and solvent content of RDX taken at point C. This figure shows that the liquid inclusion increases considerably when the initial cooling rate is higher than 0.5, 0.5, and 0.3 deg/min for the saturation temperatures of 60, 70, and 80 °C, respectively. Those values were taken as optimized cooling rates at period A−B.

After nucleation and stabilization of seed crystals, the process parameters involving reheating (period C−D) and cooling (period E−F) processes were determined as described in section 2.3. Figure 4 represents solvent content of RDX samples taken at point F at the saturation temperature of 70 °C. In this figure, the amount of liquid inclusion is shown to increase with the degree of temperature increase due to reduction of seed crystals and subsequent rapid crystal growth. Also, it is clearly shown that liquid inclusion increases when the degree of heating is larger than 2.0 °C. However, there is not any noticeable change in solvent content when the degree of heating is smaller than 2.0 °C. Figure 5 represents the crystal size and solvent content of RDX samples taken at the point F for the saturation temperatures of 60, 70, and 80 °C, when the cooling rate of 0.5 deg/min was employed. This figure also supports that the degree of temperature increase of 2 °C is reasonable at period C−D.

Figure 6 represents the effect of cooling rate at period E−F on the crystal size and solvent content of RDX crystals. As can be seen from Figure 6a, inclusion content tends to increase when the cooling rate is higher than 1.5 deg/min at the saturation temperature of 60 °C. Therefore, a cooling rate of 1.0 deg/min was taken in this experiment. This result agrees with previous reports that rapid cooling could induce a large amount of liquid inclusion.[19,28] However, opposite results were obtained for the saturation temperatures of 70 and 80 °C as shown in panels b and c of Figure 6. Those results may be explained by generation of fine particles induced by secondary nucleation. Figure 7 shows the optical micrographs of RDX samples taken at point F for the saturation temperature of 70 °C with various cooling rates at period E−F. Those figures clearly show that, when the cooling rate is higher than 1.0 deg/min (Figure 7c), very fine particles were formed and the solvent content of this sample was measured to be 700 ppm. On the other hand, when those particles were collected by sieving, it is interesting to note that the solvent content of coarse particles bigger than 150 μm was measured to be 2140 ppm and that of fine particles smaller than 150 μm was 108 ppm. Those results agree with an earlier study

dx.doi.org/10.1021/op100334y |*Org. Process Res. Dev.* 2011, 15, 602–609

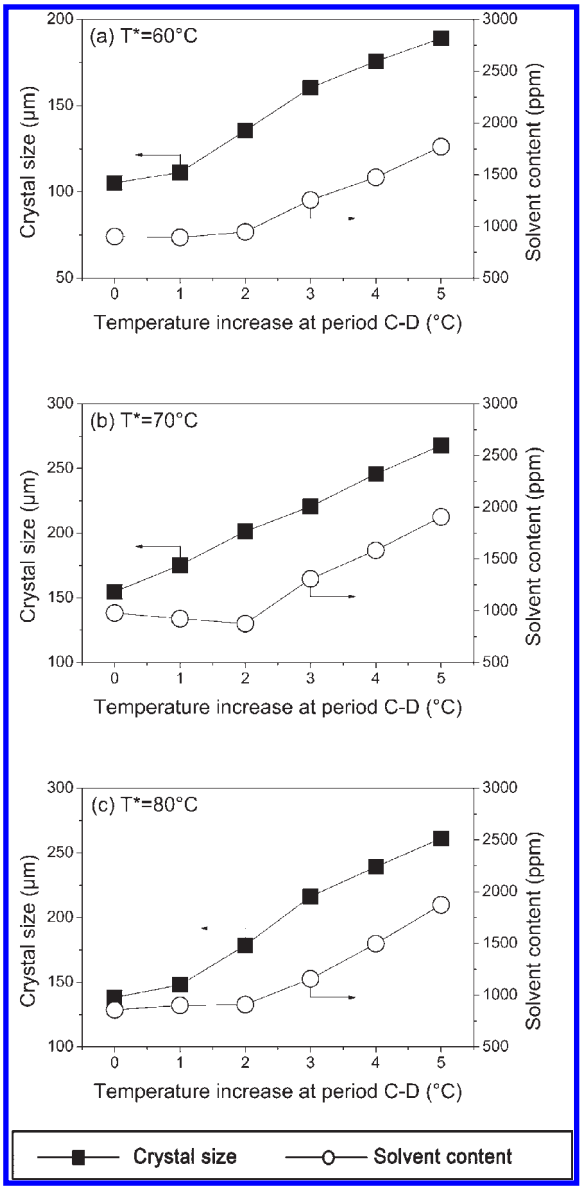

Figure 5. Size of RDX crystals and solvent content taken at point F with various temperature increases at period C−D anda cooling rate of 0.5 deg/min at period E−F.

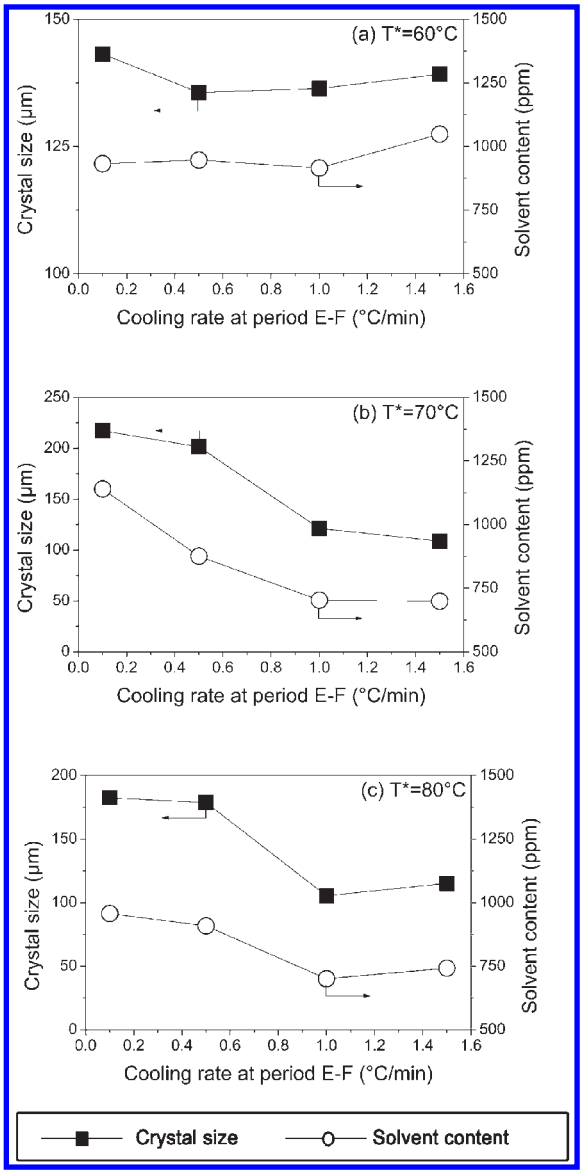

Figure 6. Size and solvent content of RDX crystals taken at point F with various cooling rates at period E−F.

on RDX by Spyckerelle et al.[33] However, smaller particles have a deleterious effect on homogeneity and flowability during the downstream process. Therefore, reconciling solvent content with crystal size, CSD, and operating time, a cooling rate of 0.5 deg/min was chosen at period E−F for the saturation temperatures of 70 and 80 °C.

3.2. Crystal Growth Stage with Temperature Cycling. For the experiments with saturation temperatures of 60 and 70 °C, two more reheating steps were applied at 39.5−43.0 and 30.0−36.0 °C (Figure 1a), and at 40.5−44.0 and 30.0−36.0 °C (Figure 1b). For the saturated solution at 80 °C, three more heating steps were applied at 64.5−66.5, 49.5−53.5, and 30.5−36.5 °C (Figure 1c).

3.3. Crystal Quality of RDX Produced by Internal Seeding and Temperature Cycling. In general, liquid inclusion tends to reduce when the growth rate of crystals is moderate. Therefore, liquid inclusion can be effectively reduced by increasing initial saturation temperature.[28] However, it has been reported that the growth rate at the crystal growth stage of RDX from γ-butyrolactone is not moderate enough to prevent the occurrence of liquid inclusion.[19] Therefore, crystallization with higher initial saturation temperature of RDX is not an effective method to reduce liquid inclusion. Figure 8 (see also Table 3) shows the comparison of crystal size and liquid inclusion between RDXs with the internal seeding and the linear cooling. Temperatures given at each data point represent initial saturation temperatures. As described above, liquid inclusion increases as initial saturation temperature increases. However, this figure clearly shows that liquid inclusion is effectively suppressed by the crystallization with the internal seeding method combined with temperature cycling without crystal size reduction compared with those with the linear cooling.

Panels a and b of Figure 9 are optical micrographs with matching refractive index of RDX crystallized by a linear cooling method at an initial saturation temperature of 90 °C and by the

dx.doi.org/10.1021/op100334y |Org. Process Res. Dev. 2011, 15, 602–609

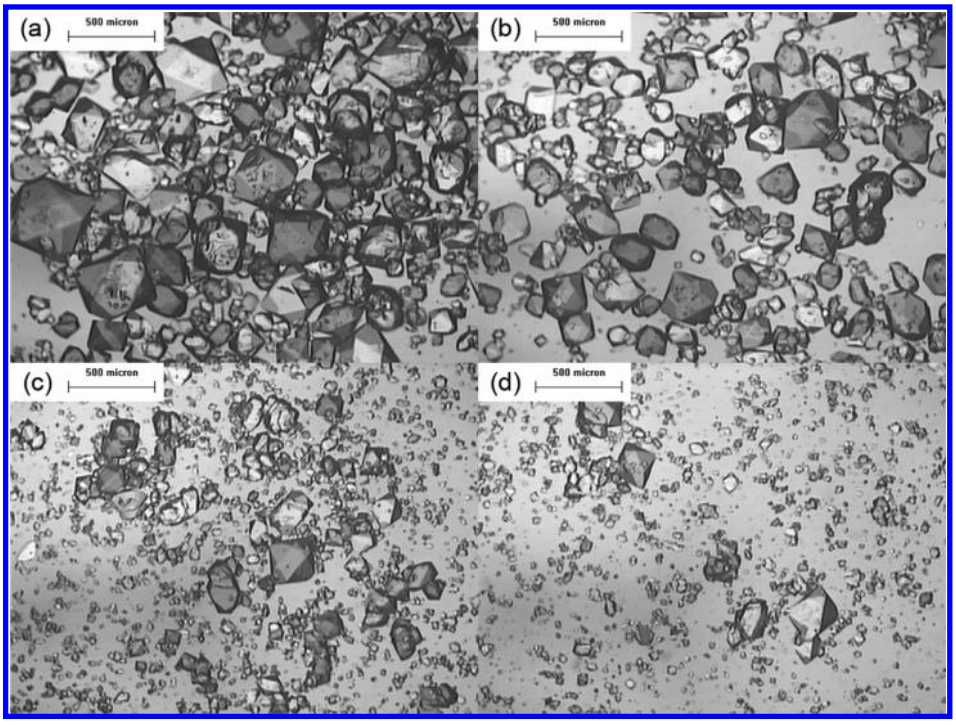

Figure 7. Optical micrographs of RDX crystals taken at point F with various cooling rates at period E−F: (a) 0.1, (b) 0.5, (c) 1.0, and (d) 1.5 deg/min (initial saturation temperature: 70 °C).

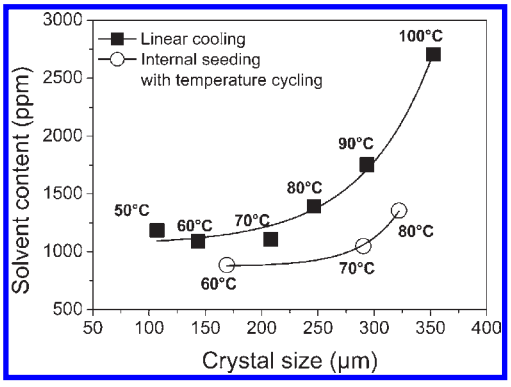

Figure 8. Influence of the cooling profile on liquid inclusion and crystal size. Temperatures indicate initial saturation temperatures.

internal seeding with temperature cycling at an initial saturation temperature of 70 °C. Their crystal sizes are nearly the same as 293.4 and 290.3 μm, respectively. However, it can be said that the crystal quality of the latter is much better than that of the former: the solvent content of the former (1750 ppm) was larger than that of the latter (1050 ppm) and average inclusion areas by image analysis were 6.0% and 4.6%, respectively.

RDX crystals obtained with internal seeding combined with temperature cycling are shown to be even better (e.g., much less liquid inclusion) than those of commercial RDXs (Figure 9c,d; see also Table 3). Average crystal size and inclusion area of Hanwha-RDX are 158.0 μm and 9.3%, respectively. The size of RDX with the internal seeding at an initial saturation temperature of 60 °C is similar, but the average inclusion area of 4.4% is much smaller. When the saturation temperatures of 70 and 80 °C were employed, RDX crystals obtained with the internal seeding are

Table 3. Experimental Results of RDX Recrystallized by Linear Cooling, Internal Seeding with Temperature Cycling, and Two Commercial RDXs (Hanwha-RDX and I-RDX)

sample	initial saturation temp (°C)	crystal size (μm)	solvent content (ppm)	inclusion area (%)
linear cooling	50	107.2	1180	5.3
	60	143.7	1090	4.7
	70	208.1	1110	5.2
	80	246.3	1390	5.5
	90	293.4	1750	6.0
	100	352.6	2700	10.9
internal seeding with temp cycling	60	169.0	885	4.4
	70	290.3	1050	4.6
	80	322.0	1360	5.3
Hanwha-RDX		158.0		9.3
I-RDX		218.0		5.0

shown to have average inclusion areas of 4.6% and 5.3%, respectively. Those values are similar to the average inclusion area of I-RDX. However, crystal sizes of those crystals (290.3 and 322.0 μm, respectively) are much larger than that of I-RDX (218.0 μm). Therefore, from all those results, it can be concluded that cooling crystallization with the internal seeding combined with temperature cycling is a very effective method to reduce liquid inclusion, which is unavoidable during industrial cooling crystallization of RDX. It is interesting to note that the shapes of RDX obtained in the present work are well-developed polygons (Figure 9a,b), while those of the commercial RDXs (Figure 9c,d) are rounded. This may be attributed to different operating

dx.doi.org/10.1021/op100334y |*Org. Process Res. Dev.* 2011, 15, 602–609

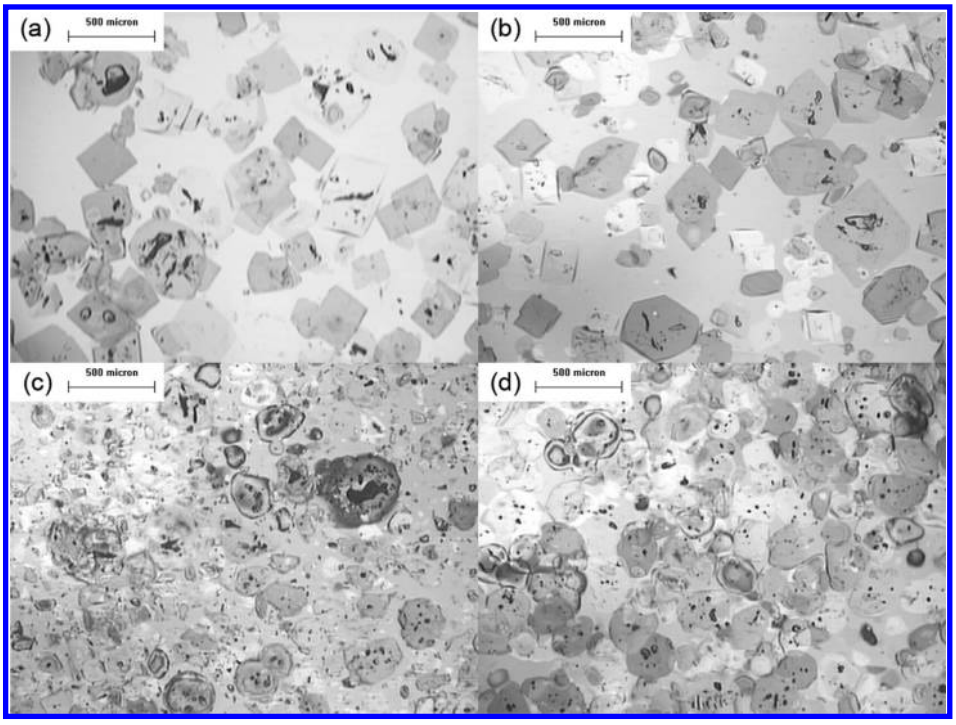

Figure 9. Optical micrographs of RDX crystals with matching refractive index: (a) initial saturation temperature of 90 °C with linear cooling, (b) initial saturation temperature of 70 °C with internal seeding and temperature cycling, (c) Hanwha-RDX, and (d) I-RDX.

conditions. Therefore, the difference in morphology among RDXs will not be discussed here.

4. CONCLUSIONS

Currently, suppression of liquid inclusion of energetic materials has been an important issue due to the relationship between internal defect and safety concerns. In the present work, the feasibility test of cooling crystallization of RDX with an internal seeding technique was performed to improve crystal quality by suppressing the occurrence of liquid inclusion during crystal growth. For the production of larger crystal size with smaller liquid inclusion, faster process time, and no fine particles, the key process parameters including initial cooling rate, the range of the temperature cycle, and recooling rates were quantitatively determined. The quality of RDX crystals obtained by the present method was found to be much better than that by a linear cooling method: for instance, crystal sizes of RDX by internal seeding with temperature cycling (temperature of saturated solution: 70 °C) and by linear cooling (temperature of saturated solution: 90 °C) are nearly the same as 290.3 and 293.4 μm, respectively. However, the inclusion area content and solvent content of the former is 4.6% and 1,050 ppm, which is much better than the latter with 6.0% and 1750 ppm, respectively. In summary, the present work clearly demonstrates that RDX crystals with reduced liquid inclusion can be produced by a typical cooling crystallization combined with internal seeding and temperature cycling. We are currently applying the proposed method to scale-up the process for RDX and crystallization of other energetic materials.

AUTHOR INFORMATION

Corresponding Author

*E-mail: koo@sogang.ac.kr. Telephone: +82-2-705-8680. Fax: +82-2-711-0439.

ACKNOWLEDGMENT

This work was supported by a Defense Acquisition Program Administration and Agency for Defense Development and Hi Seoul Science (Humanities) Fellowship from the Seoul Scholarship Foundation.

REFERENCES

(1) Paengjuntuek, W.; Kittisupakorn, P.; Arpornwichanop, A. *J. Ind. Eng. Chem.* **2008**, *14*, 442.
(2) Damour, C.; Benne, M.; Boillereaux, L.; Grondin-Perez, B.; Chabriat, J.-P. *J. Ind. Eng. Chem.* **2010**, *16*, 708.
(3) Kim, D. Y.; Paul, M.; Repke, J.-U.; Wozny, G.; Yang, D. R. *Korean J. Chem. Eng.* **2009**, *26*, 1220.
(4) Myerson, A. S. *Handbook of Industrial Crystallization*, 2nd ed.; Butterworth Heinemann: Boston, MA, 2002.
(5) Yu, Z. Q.; Chew, J. W.; Chow, P. S.; Tan, R. B. H. *Chem. Eng. Res. Des.* **2007**, *85*, 893.
(6) Doki, N.; Kubota, N.; Yokota, M.; Kimura, S.; Sasaki, S. *J. Chem. Eng. Jpn.* **2002**, *35*, 1099.
(7) Jones, A. G.; Chianese, A. *Chem. Eng. Commun.* **1987**, *62*, 5.
(8) Zipp, G. L.; Randolph, A. D. *Ind. Eng. Chem. Res.* **1989**, *28*, 1446.
(9) Sutradhar, B. C.; Randolph., A. D. *Ind. Eng. Chem. Res.* **1993**, *32*, 2781.
(10) Lewiner, F.; Févotte, G.; Klein, J. P.; Puel, F. *J. Cryst. Growth* **2001**, *226*, 348.
(11) Lewiner, F.; Févotte, G.; Klein, J. P.; Puel, F. *Ind. Eng. Chem. Res.* **2002**, *41*, 1321.
(12) Févotte, G. *Int. J. Pharm.* **2002**, *241*, 263.
(13) Chew, J. W.; Chow, P. S.; Tan, R. B. H. *Cryst. Growth Des.* **2007**, *7*, 1416.
(14) Doki, N.; Seki, H.; Takano, K.; Asatani, H.; Yokota, M.; Kubota, N. *Cryst. Growth Des.* **2004**, *4*, 949.
(15) Abu Bakar, M. R.; Nagy, Z. K.; Rielly, C. D. *Org. Process Res. Dev.* **2009**, *13*, 1343.
(16) Woo, X. Y.; Nagy, Z. K.; Tan, R. B. H.; Braatz, R. D. *Cryst. Growth Des.* **2009**, *9*, 182.

(17) Abu Bakar, M. R.; Nagy, Z. K.; Saleemi, A. N.; Rielly, C. D. *Cryst. Growth Des.* **2009**, *9*, 1378.
(18) Choi, C. S.; Prince, E. *Acta Crystallogr.* **1972**, *B28*, 2857.
(19) Kim, J.-W.; Kim, J.-K.; Kim, H.-S.; Koo, K.-K. *Cryst. Growth Des.* **2009**, *9*, 2700.
(20) Bowden, F. P.; Yoffe, Y. D. *Initiation and Growth of Explosion in Liquids and Solids*; Cambridge University Press: London, U.K., 1952.
(21) Teipei, U. *Energetic Materials*; Wiley-VCH: Weinheim, Germany, 2005.
(22) Elban, W. L.; Armstrong, R. W.; Yoo, K. C.; Rosemeier, R. G.; Yee, R. Y. *J. Mater. Sci.* **1989**, *24*, 1273.
(23) Fuhr, I.; Mikonsaari, I. Proceedings of the 2004 Insensitive Munitions & Energetic Materials Symposium, San Francisco, CA, USA, November 14−17, 2004.
(24) Kim, J.-W.; Kim, J.-K.; Kim, E. J.; Kim, H.-S.; Koo, K.-K. *Korean J. Chem. Eng.* **2010**, *27*, 666.
(25) Lee, H,-E.; Lee, T. B.; Kim, H.-S.; Koo, K.-K. *Cryst. Growth Des.* **2010**, *10*, 618.
(26) van der Heijden, A. E. D. M.; Creyghton, Y. L. M.; Marino, E.; Bouma, R. H. B.; Scholtes, J. H. G.; Duvalois, W. *Propellants, Explos., Pyrotech.* **2008**, *33*, 25.
(27) van der Heijden, A. E. D. M.; Bouma, R. H. B. *Cryst. Growth Des.* **2004**, *4*, 999.
(28) Zhang, G. G. Z.; Grant, D. J. W. *Cryst. Growth Des.* **2005**, *5*, 319.
(29) Fujiwara, M.; Chow, P. S.; Ma, D. L.; Braatz, R. D. *Cryst. Growth Des.* **2002**, *2*, 363.
(30) Nyvlt, N. *J. Cryst. Growth* **1968**, *3*, 377.
(31) Wierzbowska, B.; Piotrowski, K.; Koralewska, J.; Hutnik, N.; Matynia, A. *Korean J. Chem. Eng.* **2009**, *26*, 175.
(32) Doherty, R. M.; Watt, D. S. *Propellants, Explos., Pyrotech.* **2008**, *33*, 4.
(33) Spyckerelle, C.; Eck, G.; Sjöberg, P.; Amnéus, A.-M. *Propellants, Explos., Pyrotech.* **2008**, *33*, 14.
(34) Borne, L.; Ritter, H. *Propellants, Explos., Pyrotech.* **2006**, *31*, 482.